Suppression of the fluctuation effect in terahertz imaging using homomorphic filtering

Limin Xu (徐利民)[1,2], **Wenhui Fan (范文慧)**[1*], **and Jia Liu (刘 佳)**[1,2]

[1]*State Key Laboratory of Transient Optics and Photonics, Xi'an Institute of Optics and Precision Mechanics,*
Chinese Academy of Sciences, Xi'an 710119, China

[2]*University of Chinese Academy of Sciences, Beijing 100049, China*

[*]Corresponding author: fanwh@opt.ac.cn

To suppress the fluctuation effect due to laser power instability and terahertz radiation fluctuation, a homomorphic filtering method is proposed to process the terahertz images obtained from a pulsed terahertz raster scanning imaging system. The physical model of homomorphic filtering for terahertz imaging is established. The mathematical expressions are given with the specific physical meaning in accordance with the imaging principle. To demonstrate the effectiveness of the method, a homomorphic filtering experiment based on two raw terahertz images selected from the literature using a continuous-wave (CW) terahertz source is also performed. The effect of the method is compared with those described in the literature, and the advantages of homomorphic filtering are discussed. The pulsed- and CW-terahertz image processing results both show that in addition to suppressing the fluctuation effect, the method can also enhance target imaging.

OCIS codes: 120.6200, 300.6495, 100.2960, 100.2980.
doi: 10.3788/COL201311.081201.

Terahertz imaging has undergone rapid development since its initial stages[1−3]. In terahertz imaging, the fluctuation of gray level distribution cannot be avoided because of the fluctuation effect from the terahertz source, whether the source is pulsed or continuous wave (CW). To overcome the fluctuation effect with time, three calibration methods are generally utilized. In the first method, a second reference background image is obtained simultaneously or within a transient time scale. Afterward, the reference image is subtracted from the raw terahertz image. The result is a calibrated image with a mitigated background fluctuation effect. One example of this method is the dynamic subtraction method used in previous studies[4,5]. Generally, this method requires a large number of raw images and reference images to improve the signal-to-noise ratio (SNR) of the terahertz images. In the second method, a linear relationship between the decreased terahertz signal and the measurement time is first obtained to determine the reference background intensities at any given time. Afterward, the reference background image is subtracted from the raw terahertz image to obtain a calibrated image[6]. In the third method, the imaging object is first separated from the background to obtain a reference image for the background. The gray level at each line of the reference image is averaged to achieve a gray level estimation for each line. The estimation is then subtracted from the original image to mitigate the fluctuation effect[7]. However, these three methods increase the complexity of the imaging experimental setup. Furthermore, except for the dynamic subtraction method in which the signal and background frames are alternately captured within millisecond timescales, the other methods cannot ensure that the reference images and terahertz images have the same degrees of fluctuation.

Here, we present a modified homomorphic filtering method to simultaneously mitigate the fluctuation effect and enhance object imaging. We first establish a physical model and then demonstrate the feasibility of the principle. Afterward, based on our experimental results, the real effect of this method is illustrated. To illustrate the principle of this method in CW terahertz imaging experiments, we select two raw CW terahertz images from the literature[6,7] for homomorphic filtering. The results are then compared with those of the literature. Finally, a brief discussion on the usage and limitation of this method is given.

Homomorphic filtering is commonly used to suppress multiplicative noise, such as non-uniform illumination background, in visible images[8]. This method has been adapted to suppress the non-uniform illumination effect in medical imaging[9,10] and remote sensing[11]. However, fluctuations occur in both pulsed and CW terahertz radiation sources when a raster-scan is performed to obtain the terahertz image. The fluctuation is then transferred to the gray level distribution of the terahertz image, which results in severely degraded imaging quality.

According to the peak-to-peak amplitude terahertz imaging principle, if other kinds of additive noise are not taken into consideration, the two-dimensional (2D) gray level distribution for terahertz transmission images can be represented as the product of the terahertz radiation power $i(m, n)$ that is incident on the surface of the imaging targets and the transmission coefficient $t(m, n)$. Meanwhile, the 2D gray level distribution for terahertz reflection images can be represented as the product of the incident terahertz power $i(m, n)$ and the reflection coefficient $r(m, n)$. m and n are the coordinates of the 2D distribution in the spatial domain. The 2D distribution of the transmission coefficient or of the reflection coefficient contains information on the imaging targets. We hope to distill this information, but the fluctuation

effect of the terahertz radiation power $i(m,n)$, which acts as the multiplicative noise, blends with this information. The fluctuation effect and imaging information are coupled in the spatial domain. Therefore, these two parts are not separable in the frequency domain[8], and a mere high-pass filtering in the frequency domain will indiscriminatingly operate on the frequency components of both parts and will not achieve good results.

Using a logarithmic operation, the method of homomorphic filtering transforms multiplicative noise (which belongs to systematic noise) into additive noise. As a result, the frequency components of the terahertz radiation power $i(m,n)$ and the transmission coefficient $t(m,n)$ or reflection coefficient $r(m,n)$ can be separated. The fluctuation effect of terahertz radiation is characterized by slow spatial variations, whereas the transmission or reflection component tends to vary abruptly, particularly at the junctions of dissimilar objects. These characteristics lead to associating the low frequencies of the Fourier transform of the logarithm of terahertz images with the incident terahertz radiation $i(m,n)$ and the high frequencies with the transmittance or reflectance. These associations are rough approximations but can be used in image enhancement. Therefore, high-pass frequency domain filtering for the logarithmic image can suppress low-frequency components that correspond to the incident terahertz radiation $i(m,n)$, which contains the fluctuation effect, and simultaneously enhance high-frequency components that correspond to the edges and the texture. The edges and the texture are therefore emphasized. Meanwhile, the contrast between the imaging targets and the background is improved.

The mathematical description for the homomorphic filtering method includes five steps, which are shown in Fig. 1.

The high-pass filter function in the logarithmic-Fourier domain is defined as the homomorphic filter function $H(u,v)$. The parameters u and v are coordinates of the 2D distribution in the logarithmic-Fourier domain. The characteristic curve of $H(u,v)$ is shown in Fig. 2. The low value corresponds to the incident terahertz radiation component, whereas the high value corresponds to the transmission component or reflection component. D_0 is the approximate cut-off frequency between these two components. The curve shape can be approximated using any ideal high-pass filter, such as a Gaussian high-pass filter or a Butterworth high-pass filter. If the Gaussian high-pass filter is used, the homomorphic filter $H(u,v)$ can be expressed as

$$H(u,v) = (H_{\mathrm{H}} - H_{\mathrm{L}})\{1 - \mathrm{e}^{-c[D^2(u,v)/D_0^2]}\} + H_{\mathrm{L}}, \quad (1)$$

where D_0 is a specified nonnegative quantity, $D(u,v)$ is the distance from point (u,v) to the origin of the frequency rectangle, H_{H} is the highest point of $H(u,v)$, and H_{L} is the lowest point. The sharpness of the slope of the filter function can be controlled by adjusting the parameter c.
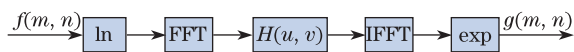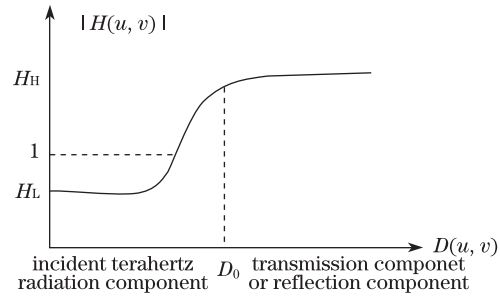

Fig. 1. Homomorphic filtering process.

Fig. 2. Homomorphic filter $H(u,v)$.

The construction of the homomorphic filter $H(u,v)$ has been discussed above. The mathematical description of homomorphic filtering for terahertz transmission imaging will be discussed as follows.

The terahertz transmission images can be expressed as Eq. (2), where $f(m,n)$ is the 2D gray level distribution of the terahertz transmission imaging.

$$f(m,n) = i(m,n) \cdot t(m,n). \quad (2)$$

Suppose, however, that we define

$$z(m,n) = \ln f(m,n) = \ln i(m,n) + \ln t(m,n). \quad (3)$$

Then,

$$\mathrm{FFT}[z(m,n)] = \mathrm{FFT}[\ln i(m,n)] + \mathrm{FFT}[\ln t(m,n)] \quad (4)$$

or

$$Z(u,v) = I(u,v) + T(u,v), \quad (5)$$

where $Z(u,v)$, $I(u,v)$, and $T(u,v)$ are Fourier transforms of $z(m,n)$, $\ln i(m,n)$, and $\ln t(m,n)$, respectively.

Then, we process $Z(u,v)$ using the homomorphic filter function $H(u,v)$ to obtain $S(u,v)$ as

$$\begin{aligned} S(u,v) =& H(u,v)Z(u,v) \\ =& H(u,v)I(u,v) + H(u,v)T(u,v). \end{aligned} \quad (6)$$

In the spatial domain,

$$\begin{aligned} s(m,n) =& \mathrm{IFFT}[S(u,v)] = \mathrm{IFFT}[H(u,v)I(u,v)] \\ &+ \mathrm{IFFT}[H(u,v)T(u,v)]. \end{aligned} \quad (7)$$

By letting

$$i'(m,n) = \mathrm{IFFT}[H(u,v)I(u,v)], \quad (8)$$

and

$$t'(m,n) = \mathrm{IFFT}[H(u,v)T(u,v)], \quad (9)$$

Equation (7) can be expressed as

$$s(m,n) = i'(m,n) + t'(m,n). \quad (10)$$

The exponential operation for $s(m,n)$ yields the desired enhanced image, which is denoted by

$$g(m,n) = \mathrm{e}^{s(m,n)} = \mathrm{e}^{i'(m,n)} \cdot \mathrm{e}^{t'(m,n)}. \quad (11)$$

The 2D gray level distribution of the homomorphic filtered images can be also expressed as

$$g(m,n) = i_0(m,n) \cdot t_0(m,n), \quad (12)$$

where $i_0(m,n)=\mathrm{e}^{i'(m,n)}$, $t_0(m,n)=\mathrm{e}^{t'(m,n)}$. $i_0(m,n)$ and $t_0(m,n)$ represent the outputs of the terahertz radiation and transmission components, respectively.

The mathematical equations can be adapted to terahertz reflection imaging simply by replacing the transmission coefficient $t(m,n)$ with the reflection coefficient $r(m,n)$.

With a homomorphic filter, a significant amount of control can be gained over the incident terahertz radiation component as well as on the transmission or reflection component. This control demands specification of a filter function $H(u,v)$ that affects the low- and high-frequency components of the logarithmic-Fourier domain in different ways. As shown in Fig. 2, if the parameters H_L and H_H are set such that $H_L<1$ and $H_H>1$, the homomorphic filter function tends to decrease the contribution made by the low frequencies while amplifying the contribution made by high frequencies. Thus, the fluctuation effect of terahertz power radiation is suppressed, whereas the transmission or reflection components representing the detailed information of imaging objects are enhanced. The net result is a simultaneous dynamic range compression and contrast enhancement.

The scan length for scanning a blade edge is set to 0.5 mm. Given that the broadband pulsed terahertz radiation source is used, the scan length cannot be set shorter than 0.3 mm. The main part of the radiation source lies in a relatively lower frequency band. Therefore, the diffraction effect will render smaller scan lengths meaningless. The pixel of the raw terahertz image is 52×50.

Figure 3 shows the homomorphic filtering and image enhancement of a blade-edge image. Figure 3(O) is the optical image of a blade-edge sample. The two local parts denoted by rectangles are the reference. Figure 3(a) is the original terahertz transmission image. According to the experimental condition, three layers should be represented in Fig. 3(a). In the first layer (from bottom to top), terahertz waves are directly transmitted without completely passing through the imaged object. In the second layer, the terahertz waves are transmitted through the cardboard, and most of the THz energy penetrates. In the third layer, the terahertz waves hit the target, but most are reflected back. However, these three layers are difficult to identify because of non-uniform illumination. In addition, the blade edges are blurred because of diffraction. The lower part of the raw image is too bright to be discerned, whereas the upper part is relatively dark. Figure 3(b) shows the result of a modified homomorphic filtering of the raw image. Figure 3(c) displays the result of high-pass Butterworth filtering of the raw image in the Fourier domain. A comparison of these two figures show that high-pass filtering in the Fourier domain is not sufficient to suppress the background fluctuation effect. Because the filter indiscriminatingly mitigates the low-frequency components of both the non-uniform background and the imaging targets, the image quality decreases further. The aforementioned three layers can be clearly seen in Figs. 3(b) and 3(c). However, the background in Fig. 3(c) is too dark. Figures 3(d) to 3(f) are the results of edge detection for Figs. 3(a) to 3(c), respectively, using the Prewitt operator[12]. A comparison of Figs. 3(d) to 3(f) with Fig. 3(O) shows that the illusory edges are eliminated in Fig. 3(e), and

the real edges of the shaver can be easily discerned. To compare the edge resolutions quantitatively, the two local parts mentioned above are selected, as shown in Fig. 4 (drawn to scale). The sizes of these two local parts are 0.75×0.40 (mm) and 0.65×0.65 (mm), respectively. A-0 and B-0 are taken from the optical image of the blade-edge sample. A-1 and B-1 are the corresponding parts from Fig. 3(d), whereas A-2 and B-2 are the corresponding parts from Fig. 3(e), respectively. The edge resolutions (measured in pixels; Table 1) shows a distinct improvement after homomorphic filtering, thus demonstrating the effectiveness of homomorphic filtering. The homomorphic filter function used in the experiment is shown in Fig. 5, with the highest value H_H at 1.2 and the lowest value H_L at 0.4.

To illustrate our method further, two raw CW terahertz images selected from the literature[6,7] are processed by our modified homomorphic filtering method. We first cut the pictures from the PDF format and then transform the raw images into the JPG format to obtain gray level distribution values. We use these values to perform the image processing experiment, as shown in Figs. 6 and 7.
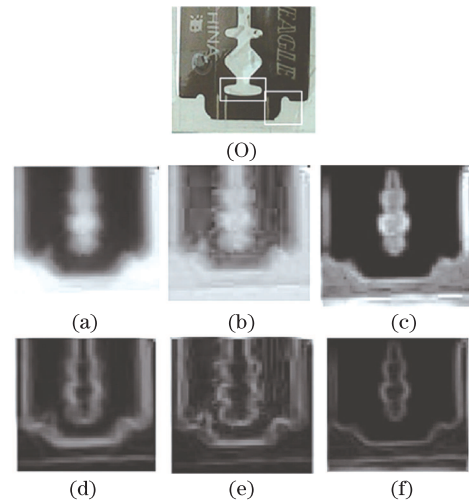

Fig. 3. Homomorphic filtering for blade-edge terahertz transmission image and enhancement. (O) Optical image of the blade-edge, (a) original experimental blade-edge image, (b) homomorphic filtering for raw image, (c) high-pass Butterworth filtering for raw image, and (d)–(f) edge detection for Figs. 3(a)–(c) using the Prewitt operator, respectively.
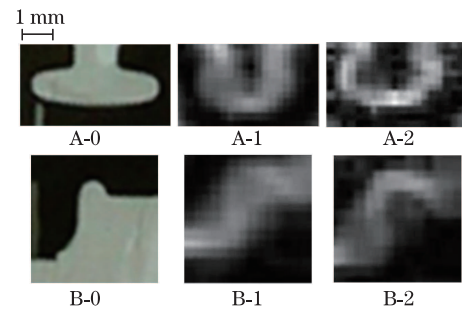

Fig. 4. Two local parts selected to demonstrate the resolution improvement of the edges. A-0 and B-0 are the two local parts selected from the image of the blade edge in Fig. 3, which are denoted by rectangles. A-1 and B-1 are the corresponding parts from Fig. 3(d), whereas A-2 and B-2 are the corresponding parts from Fig. 3(e), respectively.

Table 1. Comparison of Edge Resolutions

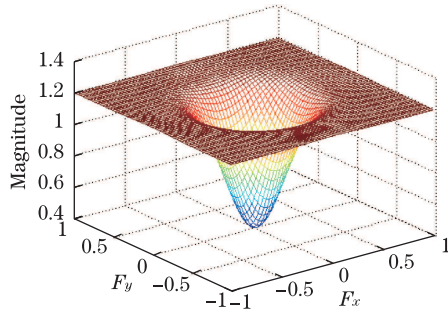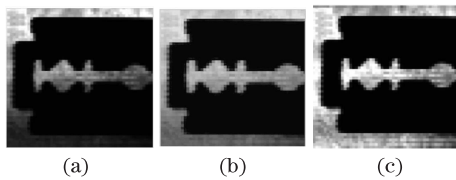| Local Part	A-1	A-2	B-1	B-2
Resolution (pixels)	4	2.3	4	2.8

Fig. 5. Homomorphic filter with H_H=1.2, H_L=0.4.

Fig. 6. Homomorphic filtering results of a blade terahertz transmission image selected from a published paper. (a) Original terahertz image, (b) image processed using our method, and (c) image processed with the background calibration method described in Ref. [6].
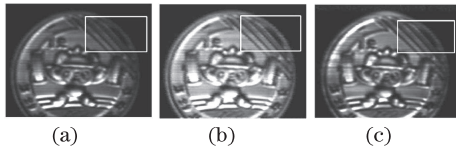

Fig. 7. Homomorphic filtering of a coin terahertz reflection image selected from a published paper. (a) Original terahertz image, (b) image processed using our method, and (c) fluctuation suppression result using the method described in Ref. [7].

Figures 6(a) and 7(a) are the raw terahertz images affected by the terahertz power fluctuation effect. The images show a clear non-uniform gray level distribution.

As described in Ref. [6], the far infrared (FIR) laser power in the experiment gradually decreases. The blade edge was raster-scanned from top to bottom. The FIR laser power drift leads to a non-uniform background in the terahertz transmission image, with a relatively brighter upper part and a darker lower part. To calibrate this power drift effect, a stability test for the laser output power was performed and a linear fit of the curve was found, which indicates a gradual decrease with time in laser power. The background gray level distribution for the transmission experiment was estimated according to this linear curve and then deducted from the raw terahertz blade-edge image. Figure 6(b) is the image processed using our method, whereas Fig. 6(c) shows the image processed with the background calibration method described in the literature[6]. H_H is set to 2 and H_L is set to 0.5 in the homomorphic filter function used in Fig.

6(b). Figure 6(b) shows a comparatively more uniform background gray level distribution as well as an improved contrast compared with that in Fig. 6(a). Moreover, the effect is nearly as good as in Fig. 6(c). A comparison of the gray level medians for the different parts (upper, middle, and lower) of the background taken from Fig. 6 is shown in Table 2. The gray level distribution for the background in Fig. 6(b) is more uniform than that in Fig. 6(a) but still not as good as in Fig. 6(c). However, the striation effect along the scanning direction due to the gradually changing laser power is severe in Fig. 6(c).

Based on the literature[7], the scanning of a coin with a 110×142 image size lasted nearly 2 hours. The long scanning time indicates that the reflection imaging result was severely affected by the laser output fluctuation. The laser power gradually changed along the scanning direction and subsequently caused striations in the raw image. Moreover, the entire reflection image was non-uniform, with the lower part relatively brighter and the upper part relatively darker. To estimate the laser output, the author first separated the object from the background to obtain a reference image and then estimated the illumination power $i(m, n)$ by averaging the gray level at each line. To suppress the laser fluctuation effect, the author removed the illumination power $i(m, n)$ from the raw reflection terahertz image. Figure 7(b) shows the image processed using our method. Figure 7(c) is the fluctuation suppression result using the method described in the literature[7]. H_H is set to 3 and H_L is set to 0.6 in the homomorphic filter function used in Fig. 7(b). Figure 7(b) clearly shows a more uniform gray level distribution than Fig. 7(a) and exhibits a better contrast than Fig. 7(c). A comparison of the imaging target-background contrast for Fig. 7 is shown in Table 3. The average gray levels for the backgrounds are approximately 3. Moreover, Table 3 gives the average (including the imaging target and background) gray levels of the different parts (from top to bottom: pixel lines 100, 200, 300, and 490; the total number of pixel lines is approximately 500). According to the gray level distribution in Table 3, we can safely conclude that the target-background contrast in Fig. 7(b) is greater than that in Figs. 7(a) and 7(c). The relatively darker parts denoted by rectangles in the top right corner of the coin can be easily identified in Fig. 7(b).

Table 2. Comparison of Gray Level (0 to 255) Medians for Different Parts of the Background in Fig. 6

	(a)	(b)	(c)
Upper Line	208	205	223
Middle Line	141	182	210
Lower Line	66	120	220

Table 3. Comparison of the Target-Background Contrast (0 to 255) in Fig. 7

	(a)	(b)	(c)
Background Gray Level	3	2.2	3.5
Average Gray Level at Line 100	19.8	42.8	32.7
Average Gray Level at Line 200	38.7	63.5	45
Average Gray Level at Line 300	38.4	72.6	48.6
Average Gray Level at Line 490	26.1	49.8	35

Our homomorphic filtering method can avoid more complicated data processing and significantly more complex experimental setups[4−7], because a reference terahertz image or background estimation is not necessary to calibrate the non-uniform terahertz radiation effect. By adjusting the parameters of the homomorphic filter function $H(u, v)$, the details of the experimental terahertz imaging can be enhanced while also improving the contrast between the imaging target and the background.

We propose a homomorphic filtering model for a terahertz imaging experiment and provide the mathematical expressions with specific physical meaning in accordance with the terahertz imaging principle. To the best of our knowledge, this letter is the first to report on the use of homomorphic filtering in terahertz imaging to suppress the fluctuation effect and enhance the imaging targets. The homomorphic filter function operates on the frequency components of terahertz images in the logarithmic-Fourier domain rather than in the Fourier domain because the fluctuation effect and the transmission or reflection components can be separated in the former domain but are blended within the entire Fourier domain. By assuming that we use the Gaussian high-pass filter in this letter, the effect of homomorphic filtering depends mainly on the choice of four homomorphic filter parameters, namely, H_H, H_L, c, and D_0. H_H is generally set to be larger than 1, and H_L is generally set between 0 and 1. The homomorphic filter operates separately on the fluctuation effect and on the information of the imaging targets, thus simultaneously suppressing the fluctuation effect and enhancing the imaging targets. The processed results of our pulsed terahertz imaging experiment as well as of two raw CW terahertz images selected from the literature have demonstrated the effectiveness of this method. The proposed method can also simplify the experimental setup as well as the data processing for fluctuation calibration compared with previous methods[4−7] because laser power stability experiments or reference background images are not necessary.

However, this method cannot significantly improve the resolution of terahertz images, which is one of the key problems that hinder the development of terahertz imaging technology[13,14]. The improvement in the SNR of the terahertz images is not as obvious as that achieved using the dynamic subtraction method[4,5] because of the presence of other types of additive noise. The dynamic subtraction method reduces the noise of raw terahertz images mainly by means of averaging, which is not adopted here. Averaging over several frames of raw experimental images is a general method utilized to smoothen the additive noise, particularly for real-time CW terahertz imaging[15]. However, obtaining several raw terahertz images requires time and even slows down the process considerably compared with the raster-scanning method when the number of raw terahertz images becomes too large. To improve the terahertz image resolution and suppress other types of noise, we still have to use other image-processing methods combined with the imaging principles. High-resolution reconstruction methods such as the Lucy-Richardson method[7,16], projection onto convex sets, maximum a posteriori estimation, maximum likelihood estimation, and others have been used to improve the resolution of imaging systems[17−20]. At present, high-resolution reconstruction for terahertz images is an interesting area of investigation.

References

1. B. B. Hu and M. C. Nuss, Opt. Lett. **20,** 1716 (1995).
2. D. M. Mittleman, R. H. Jocobsen, and M. C. Nuss, IEEE J. Sel. Top. Quantum Electron. **2,** 679 (1996).
3. D. M. Mittleman, M. Gupta, R. Neelamani, R. G. Baraniuk, J. V. Rudd, and M. Koch, Appl. Phys. B **68,** 1085 (1999).
4. Z. Jiang, X. Xu, and X. Zhang, Appl. Opt. **39,** 2982 (2000).
5. L. Zhang, N. Karpowicz, C. Zhang, Y. Zhao, and X. Zhang, Opt. Commun. **281,** 1473 (2008).
6. Y. Wang, Z. Zhao, Z. Chen, L. Zhang, K. Kang, and J. Deng, J. Infrared Millim. Waves **30,** 193 (2011).
7. S. Ding, Q. Li, R. Yao, and Q. Wang, Appl. Opt. **49,** 6834 (2010).
8. R. C. Gonzalez and R. E. Woods, *Digital Image Processing* (Publishing House of Electronics Industry, Beijing, 2007).
9. V. Jellus, W. Horger, and B. Kiefer, Magnetom Flash, 180, www.siemens.com/magnetom-world (2009).
10. P. Gorgel, A. Sertbas, and O. N. Ucan, J. Med. Syst. **34,** 993 (2010).
11. H. H. Arsenault and D. Lefebvre, Opt. Lett. **25,** 1567 (2000).
12. L. Xu, *Digital Image Processing* (in Chinese) (Science Press, Beijing, 2007).
13. S. Mickan, D. Abbott, J. Munch, X. Zhang, and T. van Doorn, Microelectron. J. **31,** 503 (2000).
14. X. Zhang, Phy. Med. Biol. **47,** 3667 (2002).
15. J. Yang, S. Yuan, and M. Zhang, Chin. Opt. Lett. **6,** 29 (2008).
16. Q. Li, Q. Yin, R. Yao, S. Ding, and Q. Wang, Opt. Eng. **49,** 037001 (2010).
17. S. C. Park, M. K. Park, and M. G. Kang, IEEE Signal Proc. Mag. **20,** 21 (2003).
18. M. K. Ng and N. K. Bose, IEEE Signal Proc. Mag. **20,** 62 (2003).
19. R. C. Hardie, K. J. Barnard, J. G. Bognar, E. E. Armstrong, and E. A. Watson, Opt. Eng. **37,** 247 (1998).
20. M. Elad and A. Feuer, IEEE Trans. Image Processing **6,** 1646 (1997).